Supplementary Information

Increased microtubule assembly rates mediate chromosomal instability in colorectal cancer cells

Norman Ertych[1,†], Ailine Stolz[1,†], Albrecht Stenzinger[2], Wilko Weichert[2,3], Silke Kaulfuß[4], Peter Burfeind[4], Achim Aigner[5], Linda Wordeman[6] & Holger Bastians[1,*]

Content:

1. Supplementary Figure Legends

Supplementary Figure S1 The expression level of EB3-GFP does not affect microtubule plus end assembly rates whereas partial repression of *CH-TOG/CKAP5* and low dose Taxol® treatment in various CRC cell lines suppresses chromosome number variability without affecting normal cell cycle progression. **a,** The average relative expression level of EB3-GFP is similar in all CRC cell lines investigated in microtubule assembly rate measurements. The relative expression levels of EB3-GFP were determined by quantifying the overall GFP fluorescence intensities in 20 individual cells. The graph shows mean values +/- SD (n=20 cells). **b**, HCT116 cells with representative high or low EB3-GFP expression levels were used to measure microtubule assembly rates. Scatter dot plots show average growth rates based on measurements of 20 microtubules per cell (mean +/- SEM, n=6 cells). No difference was seen in cells with low versus cells with high-level expression of EB3-GFP. **c**, Western blots showing protein levels for ch-TOG and α-tubulin in single cell clones derived from the indicated CRC cell lines stably expressing control or *CH-TOG/CKAP5* shRNAs. Relative ch-TOG protein levels were quantified. **d**, Karyotype analyses using CEP-FISH. Single cell clones derivative from SW620 cells expressing control or *CH-TOG/CKAP5* shRNA were grown for 30 generations and subsequently subjected to CEP-FISH analysis. The proportion of cells that deviate from the modal chromosome number of chromosome 7 and chromosome 15 was calculated (n= 100 cells). The detailed gains or losses of the chromosomes are given in

the Table S1. **e**, FACS analyses of CRC cells after treatment with low dose Taxol® show no cell cycle impairment. Single cell clones derived from the different CRC cells lines were generated in the absence (DMSO) or presence of low dose Taxol® (0.05 - 0.5 nM). Cells were grown for 30 generations and were then subjected to FACS analyses and representative cell cycle profiles are given. **f**, Karyotype analyses using CEP-FISH. SW837, SW620 or SW480 single cell clones were grown in the presence or absence of Taxol® for 30 generations and subsequently subjected to CEP-FISH analysis. The proportion of cells that deviate from the modal chromosome number of chromosome 7 and chromosome 15 were calculated (n=100 cells). The detailed gains or losses of the chromosomes are given in the Table S1.
Statistic source data for Supplementary Figure S1 can be found in the Supplementary Table S2.

Figure S2 Investigation of common genetic alterations found in CRC and implicated in chromosomal instability for their impact on microtubule dynamic parameters and chromosome number variability. **a**, Summary of examples of genetic alterations commonly found in CRC and their implications in mitotic regulation or chromosome segregation. **b**, Western blots showing the loss of *APC*, *TP53* or *CHK2* or the overexpression of *AURKA* or *PLK1* in HCT116 cells after transfection with siRNAs or cDNAs or in knockout cells, respectively. Since full-length APC is hardly detectable in HCT116 cells, we detected Axin-2/conductin, which is strongly induced upon Wnt pathway activation mediated by the loss of APC. Representative western blots are

shown and relative protein levels were quantified. **c**, Western blot detecting elevated protein levels of Aurora-A in HCT116 cells stably overexpressing *AURKA*. Three independent single cell clones were generated and further analyzed. Representative western blots are shown and relative protein levels were quantified. **d**, No difference in microtubule plus end assembly rates in monopolar and bipolar mitotic spindles. HCT116 and isogenic *CHK2* knockout cells were subjected to microtubule assembly rate measurements analyzing normal bipolar mitotic spindles in asynchronously growing cells an in monopolar spindles after treatment of cells with 67 µM monastrol for 3 hours. Scatter dot plots show average growth rates based on measurements of 20 microtubules per cell (mean +/- SEM, *t*-test, n=30 cells). **e**, Karyotype analyses of single cell clones derived from HCT116 cells stably overexpressing *AURKA*. Single cell clones were grown for 30 generations and the karyotype was determined from 100 metaphase spreads. The proportion of cells showing a deviation of the chromosome numbers from the modal within the defined time span was determined as a measure for chromosomal instability. The detailed distribution of chromosome numbers is given in the Table S1. **f**, Overexpression of *AURKA* or loss of *CHK2* does not induce supernumerary centrosomes in HCT116 CRC cells after overexpression of *AURKA* or after loss of *CHK2*. Three independent cell clones overexpressing *AURKA* or *CHK2* knockout cells (HCT116-*CHK2*$^{-/-}$) were investigated by immunofluorescence microscopy experiments, in which the number of γ-tubulin positive centrosomes in interphase cells were determined. Cells with more than two centrosomes were counted as positive. As a control, HCT116 cells were transiently transfected with a plasmid overexpressing *PLK4*, which

is known to induce centrosome hyper-amplification (mean +/- SD; n=1000 interphase cells per experiment). **g-i**, No change in other microtubule dynamic parameters in cells with increased microtubule plus end assembly rates. The indicated cell lines expressing EB3-GFP and treated with 67 µM monastrol were live imaged at a rate of one frame per 300 ms. Microtubule tips were automatically tracked using plusTipTracker software package and **g**, dynamicity, **h**, percent of time spent paused and **i**, catastrophe frequency were determined. The graphs show mean values +/- SE, t-test (n=12 cells for each measurement).

Statistic source data for Supplementary Figure S2 can be found in the Supplementary Table S2.

Figure S3 Partial repression of *CH-TOG/CKAP5* or low dose Taxol® treatment suppresses high chromosome number variability after loss of *CHK2* or *AURKA* overexpression without affecting normal cell cycle progression.

a, Western blots showing protein levels of ch-TOG and Aurora-A in HCT116 cell lines stably overexpressing *AURKA* after transient siRNA-mediated knockdown of *CH-TOG/CKAP5*. A representative western blot is shown and relative protein levels of ch-TOG were quantified. **b**, Western blots showing protein levels of ch-TOG in stable *CH-TOG/CKAP5* knockdown cell lines derived from parental HCT116 or HCT116-*CHK2*$^{-/-}$ cells. A representative western blot is shown and relative protein levels were quantified. **c**, Karyotype analyses using CEP-FISH of HCT116 and HCT116-*CHK2*$^{-/-}$ single cell clones grown in the presence or in the absence of 0.2 nM Taxol® for 30 generations.

The proportion of cells that deviate from the modal chromosome number of chromosome 7 and chromosome 15 were calculated (n= 100 cells). The detailed gains or losses of the chromosomes are given in the Table S1. **d**, Partial loss of *CH-TOG/CKAP5* does not affect normal cell cycle progression. Single cell clones were subjected to FACS analyses and representative cell cycle profiles are given. **e**, Low dose Taxol® does not affect normal cell cycle progression in cells after treatment with low dose Taxol®. Single cell clones derived from HCT116 cells overexpressing *AURKA* (clone 1) or derived from HCT116-*CHK2*$^{-/-}$ cells were generated in the presence of DMSO or 0.2 nM Taxol®. After 30 generations cells were subjected to FACS analyses and representative cell cycle profiles are given.

Statistic source data for Supplementary Figure S3 can be found in the Supplementary Table S2.

Figure S4 Enhanced microtubule assembly rates and impaired error correction are separable mechanisms. **a**, Determination of microtubule turnover. Examples time-lapse fluorescent images of spindles of HCT116 cells before (-6.0 s) and at the indicated times (s) after activation (Post-PA) of GFP-tubulin fluorescence. Scale bar, 5 µm. **b**, Normalized fluorescence intensity over time after photoactivating spindles of HCT116 cells overexpressing *AURKA* (clones 1 and 2). Datapoints represent mean +/- SE, n = 9-14 cells. **c**, Normalized fluorescence intensity over time after photoactivating spindles of HCT116-*CHK2*$^{-/-}$ cells after treatment with DMSO or 0.2 nM Taxol®. Datapoints represent mean +/- SE, n = 13-14 cells. **d**, Quantification of the proportion of HCT116-*CHK2*$^{-/-}$ cells showing lagging

chromosomes after transfection with luciferase or siRNAs targeting *MCAK* after washout of monastrol and after prolonging metaphase by MG132 treatment. The graph shows mean values +/- SD (*t*-test, n= 400 anaphase cells). **e**, Representative western blots showing the loss of *MCAK* in HCT116 cells after transfection with siRNAs. **f**, HCT116 cells showing a siRNA mediated loss of *MCAK* were used to determine microtubule plus end assembly rates. Scatter dot plots show average growth rates based on measurements of 20 microtubules per cell (mean +/- SEM, n=20 cells). Repression of *MCAK* does not alter microtubule plus end assembly rates. **g**, Representative western blots showing protein levels for MCAK in different CRC cells lines overexpressing human *MCAK*. **h**, Different CRC cells overexpressing *MCAK* were used to determine microtubule plus end assembly rates. Scatter dot plots show average growth rates based on measurements of 20 microtubules per cell (mean +/- SEM, n=20 cells). No difference in plus end assembly rates were found in cells overexpressing *MCAK*. **i**, Determination of microtubule plus end assembly rates in HCT116 cells after release from monastrol and after release from monastrol into MG132 to prolong the time for error correction. Scatter dot plots show average growth rates based on measurements of 20 microtubules per cell (mean +/- SEM, n=10 cells). **j**, Determination of kinetochore-microtubule turnover in HCT116 cells expressing PA-GFP-tubulin immediately after establishing bipolar spindles upon release from a monastrol block and after release from monastrol into MG132 to prolong time for error correction. The graph displays normalized fluorescence intensities over time after

photoactivation of spindles in HCT116 cells (mean +/- SE, n=33 cells for each condition).

Statistic source data for Supplementary Figure S4 can be found in the Supplementary Table S2.

Figure S5 Overexpression of *AURKA* or loss of *CHK2* in CRC cell lines results in elevated levels of active Aurora-A at mitotic centrosomes and an increased phosphorylation of the Aurora-A target protein TACC3. **a**, Representative western blots showing Aurora-A (left panel) and Chk2 (right panel) protein levels in the indicated CRC cell lines. Relative protein levels were quantified. Note that chromosomally instable CRC cells exhibiting enhanced microtubule growth rates show preferentially either an overexpression of *AURKA* or a loss of *CHK2* and these lesions correlate with increased microtubule growth rates and chromosomal instability. **b**, Overexpression of *AURKA* causes an increase in active Aurora-A (auto-phosphorylated at threonine-288) at mitotic centrosomes. Active Aurora-A was detected in HCT116 prometaphase cells stably overexpressing *AURKA* using phospho-specific antibodies in immunofluorescence microscopy experiments. Signal intensities for active Aurora-A (pT288) at mitotic centrosomes normalized to signals obtained for centrosomal centrin are depicted as 3D surface plots and quantified (mean, +/-95%-CI, *t*-test, 26-46 cells). **c**, Increased phosphorylation of TACC3 upon overexpression of AURKA in HCT116 cells. Representative western blots showing protein levels of Aurora-A, Chk2, TACC3 and TACC3 phosphorylated at Ser-558 in HCT116 cells stably overexpressing *AURKA*. Cells were synchronized in mitosis by

treatment with DME for 16 hours. Relative protein levels were quantified. **d**, Representative western blots showing increased levels of phosphorylated TACC3 in *CHK2* deficient cells on western blots. Relative protein levels were quantified. **e**, Determination of the antibodies used to detect phosphorylated Aurora-A and TACC3. Representative western blots detecting total and active forms of Aurora-A kinases after specific inhibition of Aurora-A or Aurora-B. HCT116 cells were synchronized in mitosis by nocodazole. Subsequent treatment with MG132 prevents exit from mitosis as verified by FACS analyses. Mitotic indices and relative protein levels are shown. Treatment of cells with 0.5 μM of the Aurora-A inhibitor MLN8054, but not with 2 μM of the Aurora-B inhibitor ZM447439 abolishes Aurora-A, but not Aurora-B activity as shown by detecting the active, auto-phosphorylated forms of the kinases. **f**, Treatment of mitotic cells with 0.5 μM MLN8054 abolishes centrosomal signals for the active (Thr-288 phosphorylated) form of Aurora-A. HCT116 cells were treated with DME for 3.5 h and subsequently treated with DMSO or 0.5 μM MLN8054 for additional 30 min. Total and active (P-Thr-288) Aurora-A was detected at mitotic centrosomes by immunofluorescence microscopy (active Aurora-A, red; total Aurora-A, green; DNA, blue; scale bar, 10 μm). **g**, Specificity of the antibodies used to detect the Aurora-A mediated phosphorylation of TACC3. HCT116 cells were transfected with the indicated siRNAs and synchronized in mitosis by DME treatment and subsequently treated with DMSO or 0.5 μM MLN8054. TACC3 or phosphorylated TACC3 as well as Aurora-A and the active form of Aurora-A were detected on western blots. Representative western blots are shown and relative protein levels were quantified. Both, the activity of Aurora-A and the phosphorylation of TACC3 is

abolished after inhibition of Aurora-A by MLN8054. Moreover, repression of TACC3 by siRNAs also suppressed the protein levels of total and phosphorylated TACC3, but did not affect the level of Aurora-A. Note that the phosphorylation of TACC3 and the activity of Aurora-A is high in mitotic cells and low in asynchronously growing cells.

Statistic source data for Supplementary Figure S5 can be found in the Supplementary Table S2.

Figure S6 Loss of *CHK2* or loss the Chk2-mediated phosphorylation of Brca1 causes enhanced interaction of Brca1 with active Aurora-A. **a**, Representative western blots showing the re-expression of wild type (WT), non-phosphorylatable (S988A) and phospho-mimetic (S988E) mutants of Brca1 in HCT116 cells stably expressing shRNAs targeting endogenous *BRCA1*. Relative protein levels were quantified. **b**, The interaction of Brca1 with active Aurora-A is increased when Chk2 is decreased. Immunoprecipitation of Brca1 from whole cell lysates derived from HCT116 cells with or without low levels of Chk2 (mediated by stable expression of shRNAs targeting *CHK2*) or after reconstitution of *CHK2* expression (mediated by stable expression of shRNA resistant mutant of *CHK2*). Cells were synchronized in mitosis, Brca1 was immunoprecipitated and associated Aurora-A and active Aurora-A proteins (autophosphorylated at threonine-288; P-Aurora-A) were subsequently detected on western blots. Active Aurora-A bound to Brca1 is significantly enhanced when *CHK2* expression is repressed. Representative western blots are shown and similar results were also obtained using HCT116-*CHK2*$^{-/-}$ cells (data not shown). **c**, The interaction of Brca1 with active Aurora-A is increased

after loss of the Chk2 phosphorylation site of Brca1. Immunoprecipitation of Brca1 from mitotic synchronized, stable HCT116 + *BRCA1* shRNA cells expressing either a wild type (WT), a non-phosphorylatable mutant (S988A) or a phospho-mimetic mutant (S988E) of *BRCA1* and subsequent detection of active Aurora-A (P-Aurora-A, P-Thr288). Brca1, which cannot be phosphorylated by Chk2 shows an enhanced interaction with the active form of Aurora-A. Representative western blots are shown. **d**, Control immunoprecipitation experiments showing that the interaction of Aurora-A with its co-factor TPX2 is not altered in the absence of *CHK2*. Immunoprecipitation of TPX2 from *CHK2* proficient (HCT116) or deficient (HCT116-*CHK2*$^{-/-}$) mitotic synchronized cells and subsequent detection of Aurora-A and active Aurora-A (P-Thr288) on western blots. Representative western blots are shown. Statistic source data for Supplementary Figure S6 can be found in the Supplementary Table S2.

Figure S7 Partial loss of *AURKA* in CRC cell lines restores normal mitotic progression, kinetochore microtubule turnover and chromosomal stability without affecting normal cell cycle progression. **a**, Representative western blots showing reduced protein levels of Aurora-A in *CHK2* knockout cells stably expressing *AURKA* shRNAs. Relative protein levels were quantified. **b**, Representative western blots showing reduced phosphorylation of TACC3 (P-Ser-558) in *CHK2* deficient HCT116 cells after partial loss of *AURKA*. Relative protein levels were quantified. **c**, Partial loss of *AURKA* in *CHK2* deficient cells does not affect normal cell cycle progression. Stable cell lines expressing shRNAs targeting *AURKA* were generated and subjected to FACS

analyses. Representative cell cycle profiles are shown. The cell cycle distribution is indistinguishable from the control cells. **d**, Partial loss of *AURKA* in *CHK2* deficient cells restores normal mitotic timing. The time from nuclear envelope breakdown (NEB) to anaphase onset was determined by live cell microscopy. The box and whisker plot shows the range, median and quartile of the measurements (*t*-test, n=59-163 cells per group). **e**, Partial loss of *AURKA* de-stabilizes hyper-stable kinetochore-microtubule attachments in cells with increased microtubule assembly rates. The indicated cell lines expressing photoactivatable GFP-tubulin (PA-GFP-tubulin) were used to determine the half-life of kinetochore-microtubule turnover and a summary of the measurements is given. **f**, Determination of microtubule turnover in *CHK2* deficient cells after partial loss of *AURKA*. The graph displays normalized fluorescence intensities over time after photoactivation of spindles in HCT116-CHK2-/- and cells expressing shRNAs targeting AURKA (clone 1). The graph shows mean values +/- SE (n=8-9 cells). **g**, Karyotype analyses of *CHK2* deficient HCT116 cells after partial repression of *AURKA* using CEP-FISH. Single cell clones derived from HCT116-*CHK2*$^{-/-}$ cells expressing control or *AURKA* shRNAs were grown for 30 generations and subsequently subjected to CEP-FISH analysis. The proportion of cells that deviate from the modal chromosome number of chromosome 7 and chromosome 15 were calculated (n= 100 cells). The detailed gains or losses of the chromosomes are given in the Supplementary Table S1. **h**, Representative western blots showing the protein levels of Aurora-A and the phosphorylated form of TACC3 (P-Ser-558) in various CRC cell lines stably expressing control or shRNAs targeting *AURKA*. Relative protein levels were quantified. Partial repression of *AURKA*

is accompanied with a reduction of TACC3 phosphorylation indicating a functional suppression of Aurora-A kinase at centrosomes. **i**, Karyotype analyses of SW620 cells after partial repression of *AURKA* using CEP-FISH. Single cell clones derived from SW620 cells expressing control or *AURKA* shRNAs were grown for 30 generations and subsequently subjected to CEP-FISH analysis. The proportion of cells that deviate from the modal chromosome number of chromosome 7 and chromosome 15 were calculated (n= 100 cells). The detailed gains or losses of the chromosomes are given in the Table S1.

Statistic source data for Supplementary Figure S7 can be found in the Supplementary Table S2.

Figure S8 Restoration of normal microtubule assembly rates and chromosomal stability by partial repression of *AURKA* or *CH-TOG* accelerates CRC tumor growth *in vitro* and *in vivo* without interfering with normal cell cycle progression. **a,** Accelerated colony formation activity of SW620 cells after partial loss of *CH-TOG*. Stable cell lines expressing control or *CH-TOG* shRNAs were subjected to colony formation assays in soft agar (2,000 cells per well) and colonies were counted. Graphs show mean values +/- SEM, *t*-test (n=3 experiments). **b,** Determination of colony formation in soft agar of *CHK2* deficient HCT116 cells after partial loss of *AURKA*. Stable cell lines expressing control or *AURKA* shRNAs as well as parental HCT116 cells were subjected to colony formation assays in soft agar (5,000 cells per well) and colonies were counted. Graphs show mean values +/- SEM, *t*-test (n=5 experiments). **c,** Determination of colony formation in soft agar of SW620 cells

after partial loss of *AURKA.* Stable cell lines expressing control or *AURKA* shRNAs were subjected to colony formation assays in soft agar (2,000 cells per well) and colonies were counted. Graphs show mean values +/- SEM, *t*-test (n=4 experiments). **d,** Growth of xenograft tumors derived from SW620 cells with or without partial repression of *CH-TOG/CKAP5*. Cells were injected s.c. into both flanks of the mice and tumor volumes were determined over time (mean +/- SEM, n=14-16). The experiment shown is an extension to the experiment shown in Figure 7c using an independent *CH-TOG/CKAP5* shRNA expressing clone. **e,** Growth of xenograft tumors derived from SW620 cells with or without partial repression of *AURKA*. Cells were injected s.c. into both flanks of the mice and tumor volumes were determined (mean +/- SEM, n=5-8). The experiment shown is an independent extension to the experiment shown in Figure 7d and additional clones were used. **f**, Growth of xenograft tumors derived from HCT116-*CHK2*$^{-/-}$ cells with or without partial repression of *AURKA*. Cells were injected s.c. into both flanks of the mice and tumor volumes were determined (mean +/- SEM, n=14-16). The experiment shown is an independent extension to the experiment shown in Figure 7e and additional clones were used. **g,** Xenograft tumor maintain the partial repression of *AURKA in vivo*. Cells were re-isolated from three different SW620 xenograft tumors grown in three different mice and expressing control (clone 1) or *AURKA* shRNAs (clone 1). Cells were lysed and subjected to western blotting detecting the protein levels of Aurora-A. Representative western blots are shown and relative protein levels were quantified. **h**, Tumor cells re-isolated from xenograft tumors do not show gross alterations in cell cycle distribution. Cells re-isolated from the different xenograft tumors were

subjected to FACS analyses and representative cell cycle profiles are shown. **i**, The suppression of CIN is maintained in xenograft tumors *in vivo*. Tumor cells re-isolated from xenograft tumors were subjected to karyotype analyses. The reduced degree of chromosome number variability in SW620 cells with reduced *AURKA* expression was maintained throughout the experiment (see also Supplementary Table S1 for details on the chromosome number variability).

Statistic source data for Supplementary Figure S8 can be found in the Supplementary Table S2.

2. Supplementary Table Legends

Table S1:

Summary of karyotype analyses. For each experiment the numbers of individual chromosomes per metaphase spread were determined and are listed as indicated. For the CEP-FISH analyses the gains and losses of chromosomes 7 and 15 were determined and are listed for each experiment as indicated.

3. Supplementary Movie Legends

Movie S1: Time-lapse fluorescence microscopy movie showing an example of an asynchronously growing HCT116 cell expressing GFP-tagged H2B and RFP-tagged tubulin and progressing through mitosis. The cell shows a correct spindle assembly and geometry and a timely progression through mitosis (red; mCherry-α–tubulin ; green; pEGFP-H2B). Images with 12 z-stacks were recorded every 2 minutes, deconvolved and maximal projections are shown. The movie has a speed of 5 frames per second. The scale bar represents 15 µm.

Movie S2: Time-lapse fluorescence microscopy movie showing an example of an asynchronously growing HCT116-*CHK2*$^{-/-}$ cell expressing GFP-tagged H2B and RFP-tagged tubulin during mitosis The cell shows a transient abnormalities in spindle structure and geometry associated with lagging chromosomes appearing during anaphase (red; mCherry-α–tubulin ; green; pEGFP-H2B). Images with 12 z-stacks were recorded every 2 minutes, deconvolved and maximal projections are shown. The movie has a speed of 5 frames per second. The scale bar represents 15 µm.

Movie S3: Time-lapse fluorescence microscopy movie showing an example of an asynchronously growing HCT116 cell expressing RFP-tagged H2B and GFP-tagged centrin during mitosis. The cell shows the separation of the centrioles during prophase and prometaphase (red; pcDNA-RFP-ruby-H2B; green; pEGFP-Centrin). At the time point when centrosome separation was

maximal this kind of movie was used to calculate the spatial positioning of the centrosomes as depicted in supplementary Figure 3d. Images with 14 z-stacks were recorded every minute, deconvolved and maximal projections are shown. The movie has a speed of 5 frames per second. The scale bar represents 15 µm.

Movie S4: Time-lapse fluorescence microscopy movie showing an example of an asynchronously growing HCT116-*CHK2*$^{-/-}$ cell expressing RFP-tagged H2B and GFP-tagged centrin and progressing through mitosis. The cell shows the separation of the centrioles during prophase and prometaphase, which is not significantly altered when compared to the parental cell shown in Movie S3 (red; pcDNA-RFP-ruby-H2B; green; pEGFP-Centrin). At the time point when centrosome separation was maximal this kind of movie was used to calculate the spatial positioning of the centrosomes as depicted in supplementary Figure 3d. Images with 14 z-stacks were recorded every minute, deconvolved and maximal projections are shown. The movie has a speed of 5 frames per second. The scale bar represents 15 µm.

Supplementary Figure S1

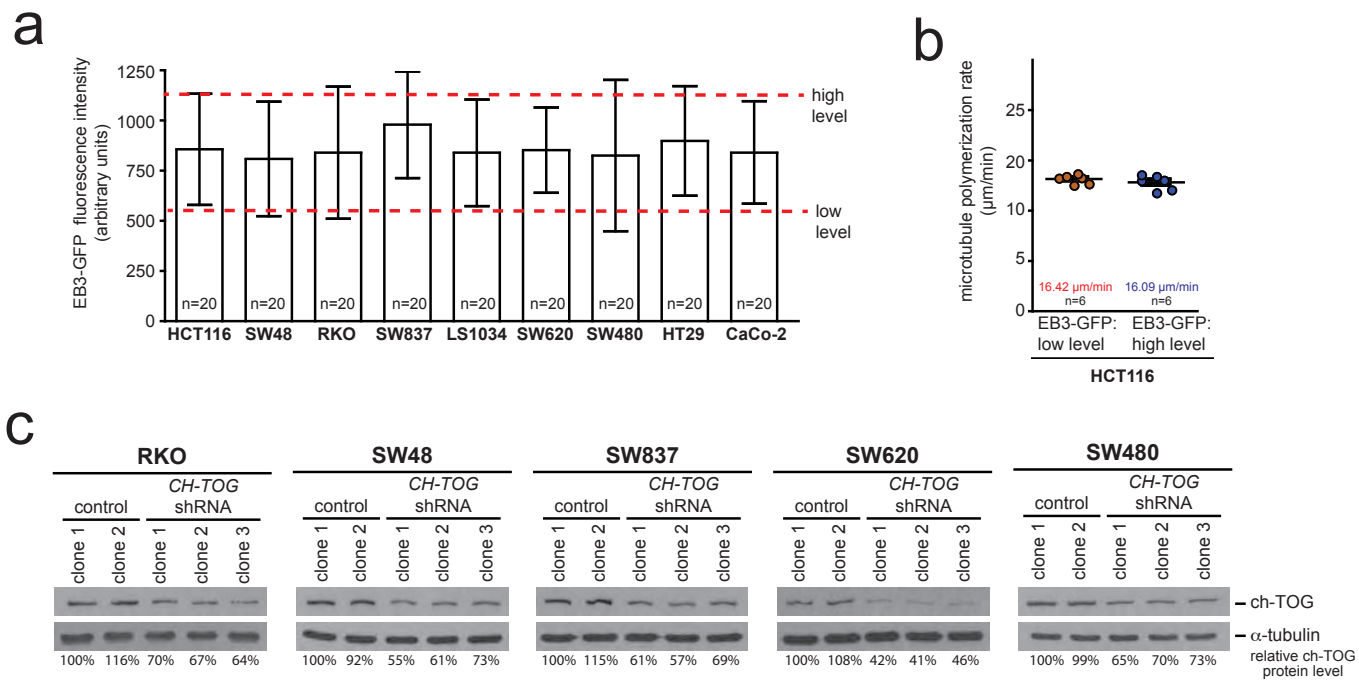

Supplementary Figure S2

a

Gene	Frequency of alteration in CRC	Association with mitosis or chromosome instability	References
APC	85% (loss)	microtubule regulation chromosome alignment	Markowitz et al., 2009; Kaplan et al., 2001
TP53	35-55% (loss)	activated after missegregation and mitotic failure	Markowitz et al., 2009; Vogel et al., 2004
KRAS	35-45% (mutated)	mitotic progression synthetic lethal with *PLK1*	Markowitz et al., 2009; Luo et al., 2009
PLK1	60-70% (overexpressed)	centrosome function mitotic spindle assembly	Weichert et al., 2005; Lens et al., 2010
AURKA	20-50% (overexpressed)	centrosome function mitotic spindle assembly	Bischoff et al., 1998; Lens et al., 2010; this study
CHK2	47% (loss)	spindle assembly chromosomal instability	Stolz et al., 2011; this study

b

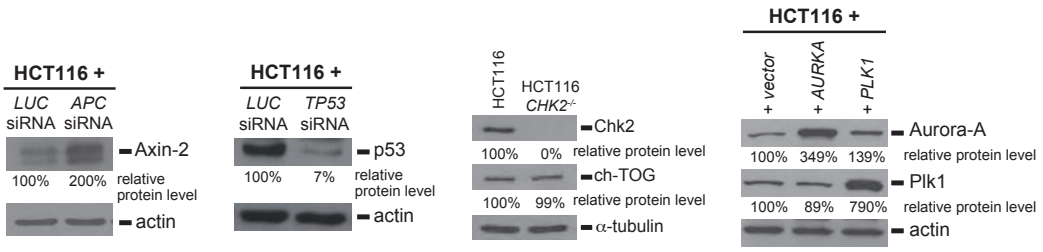

c

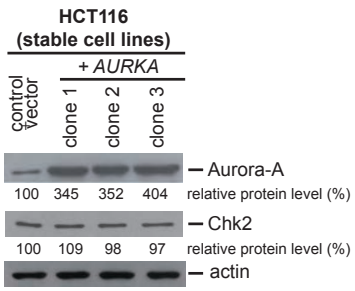

d

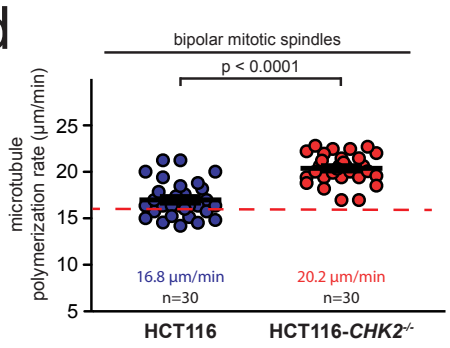

e

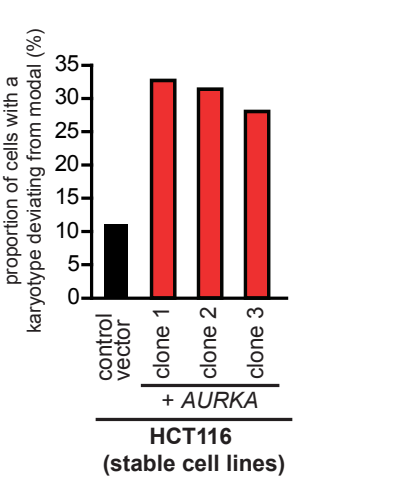

f

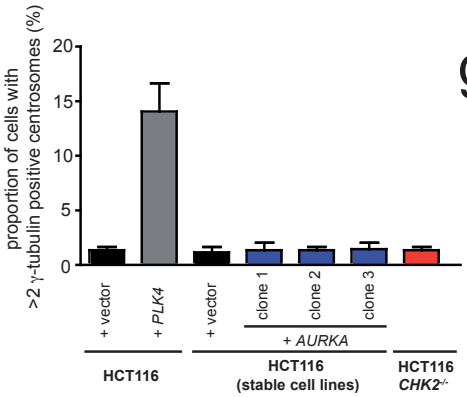

g

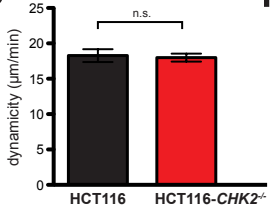

h

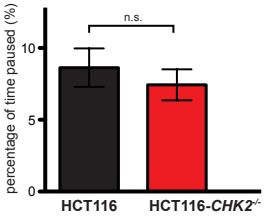

i

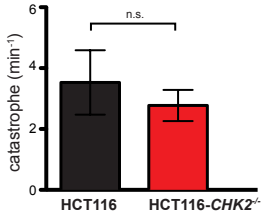

Supplementary Figure S3

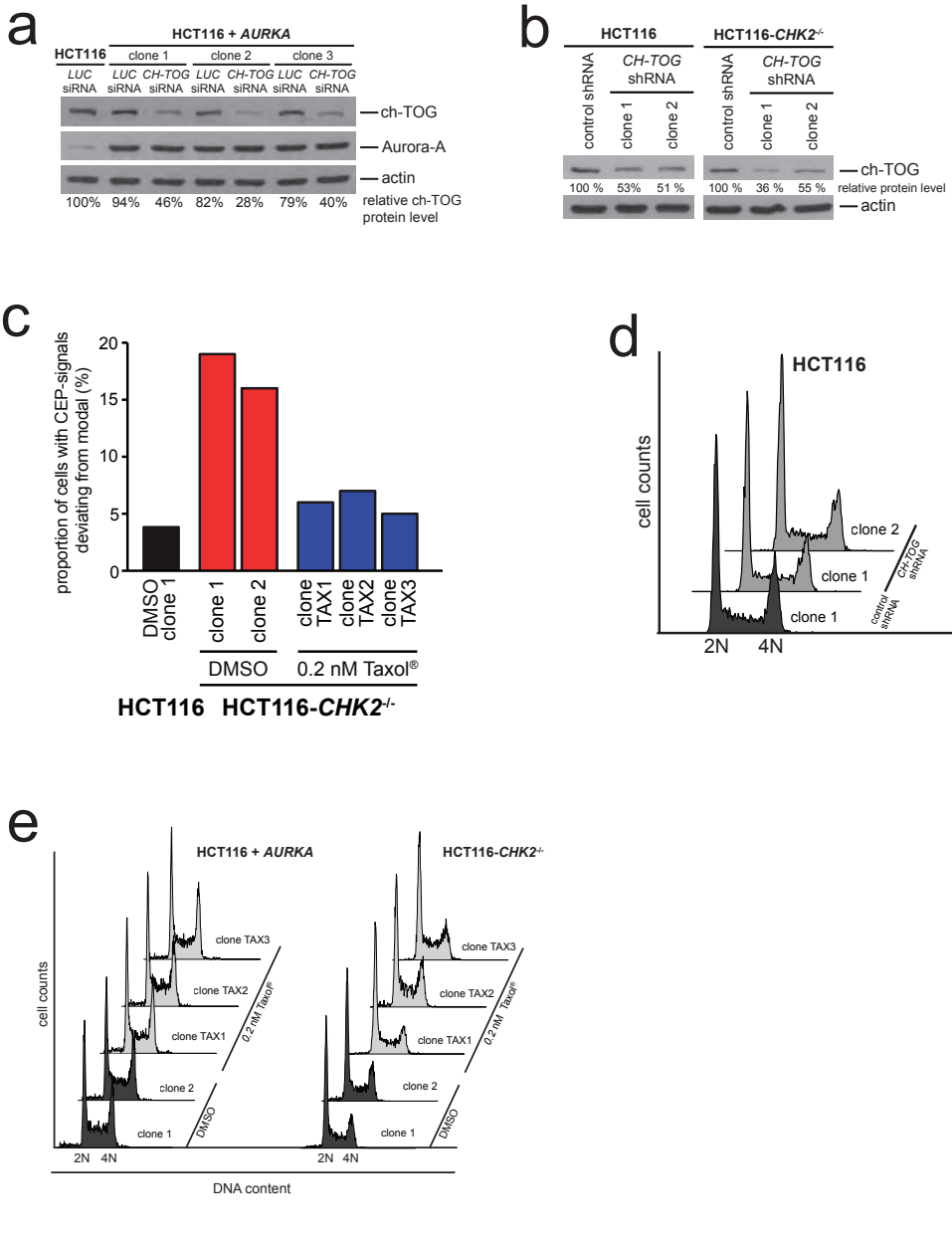

Supplementary Figure S4

new figure from Linda ???

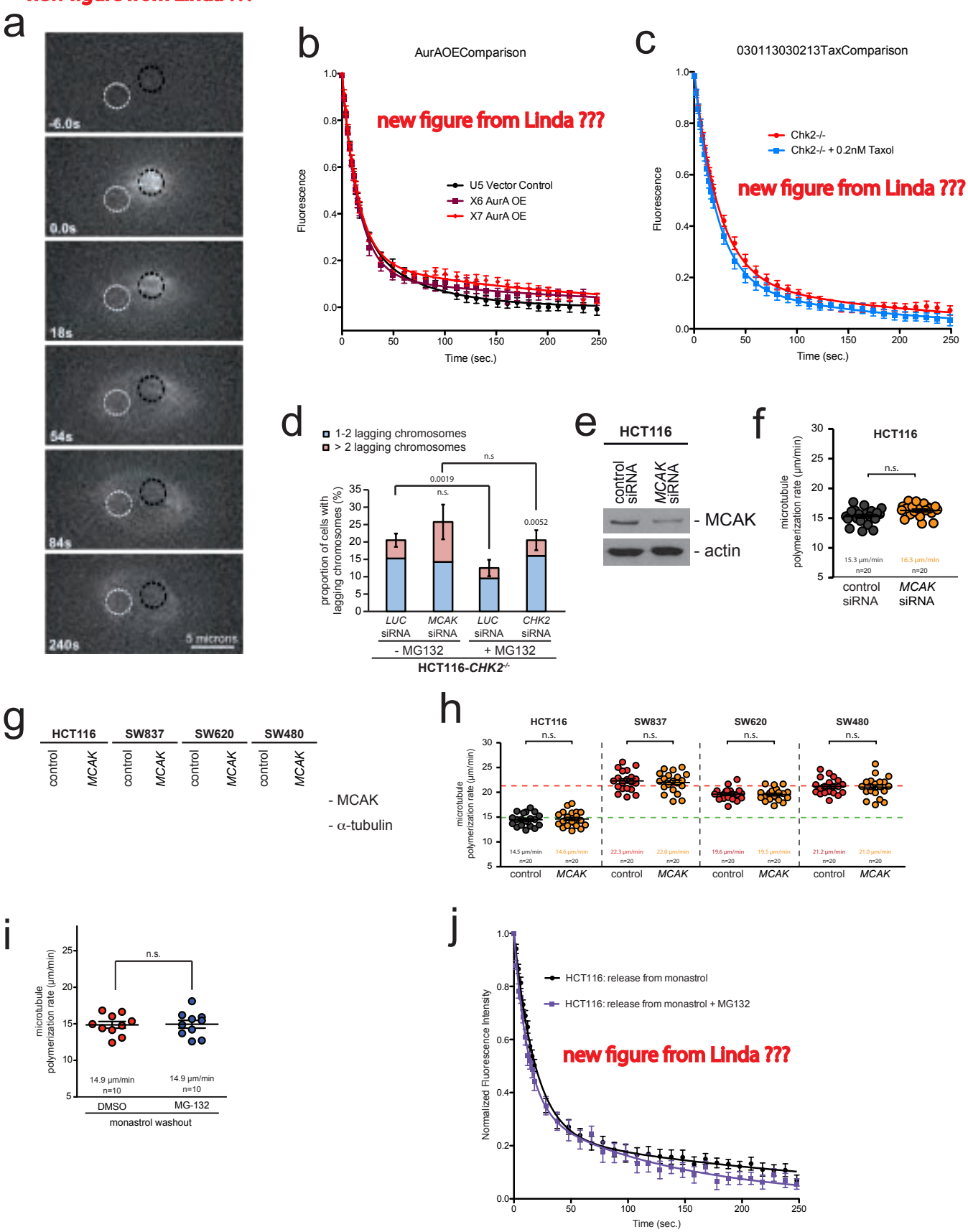

Supplementary Figure S5

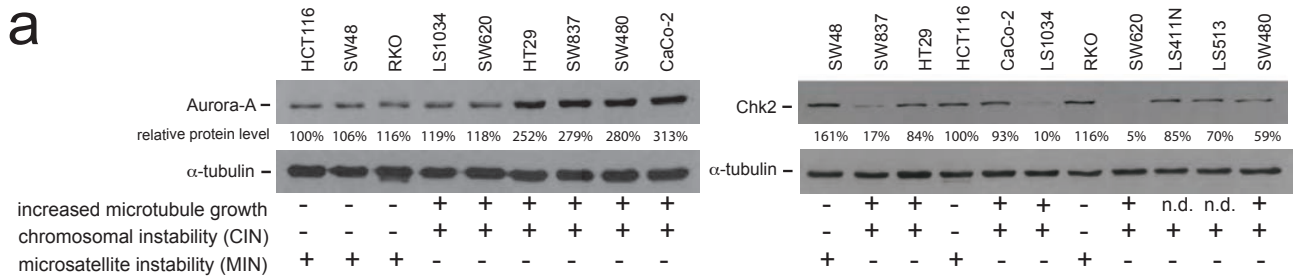

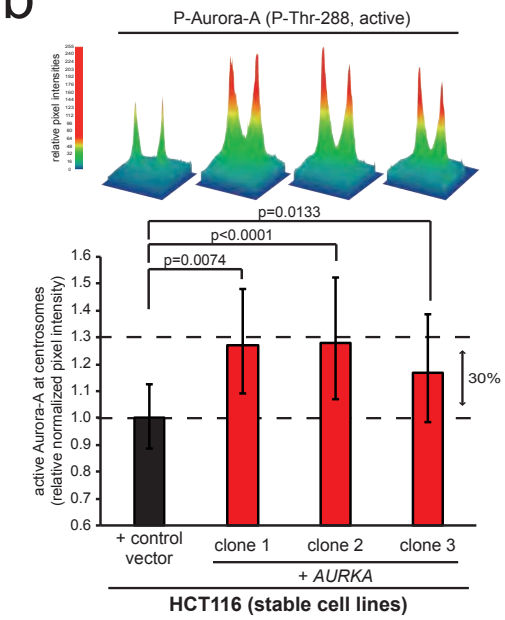

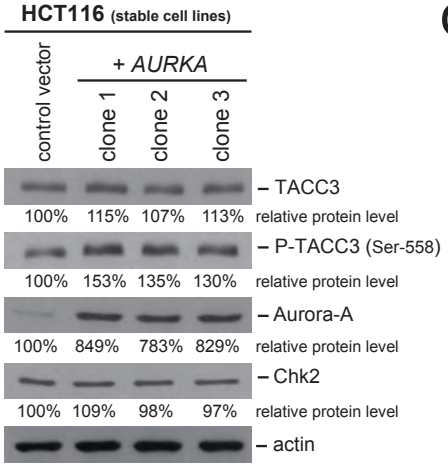

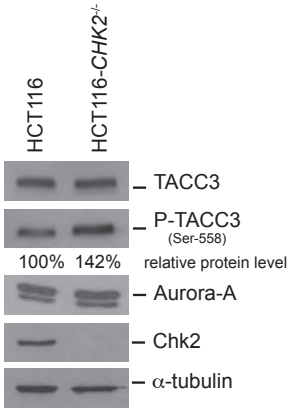

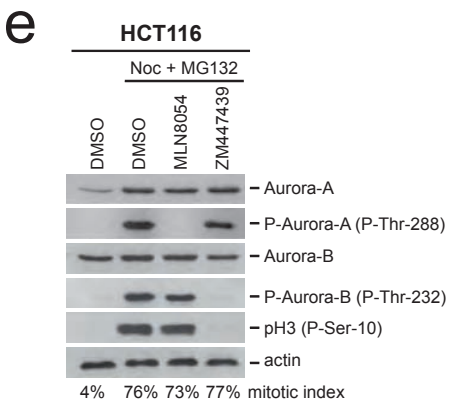

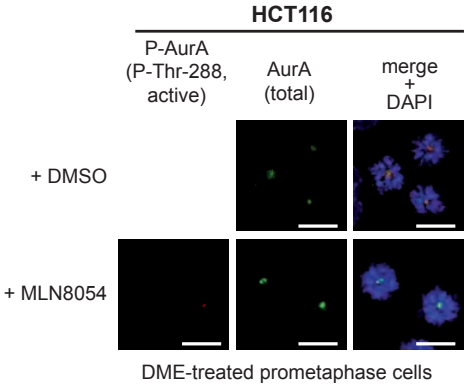

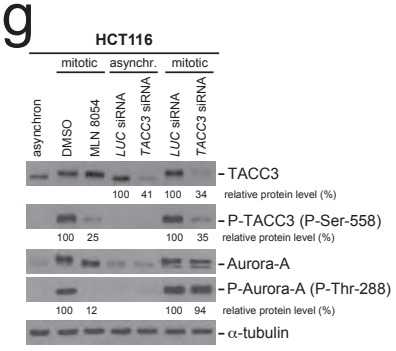

Supplementary Figure S6

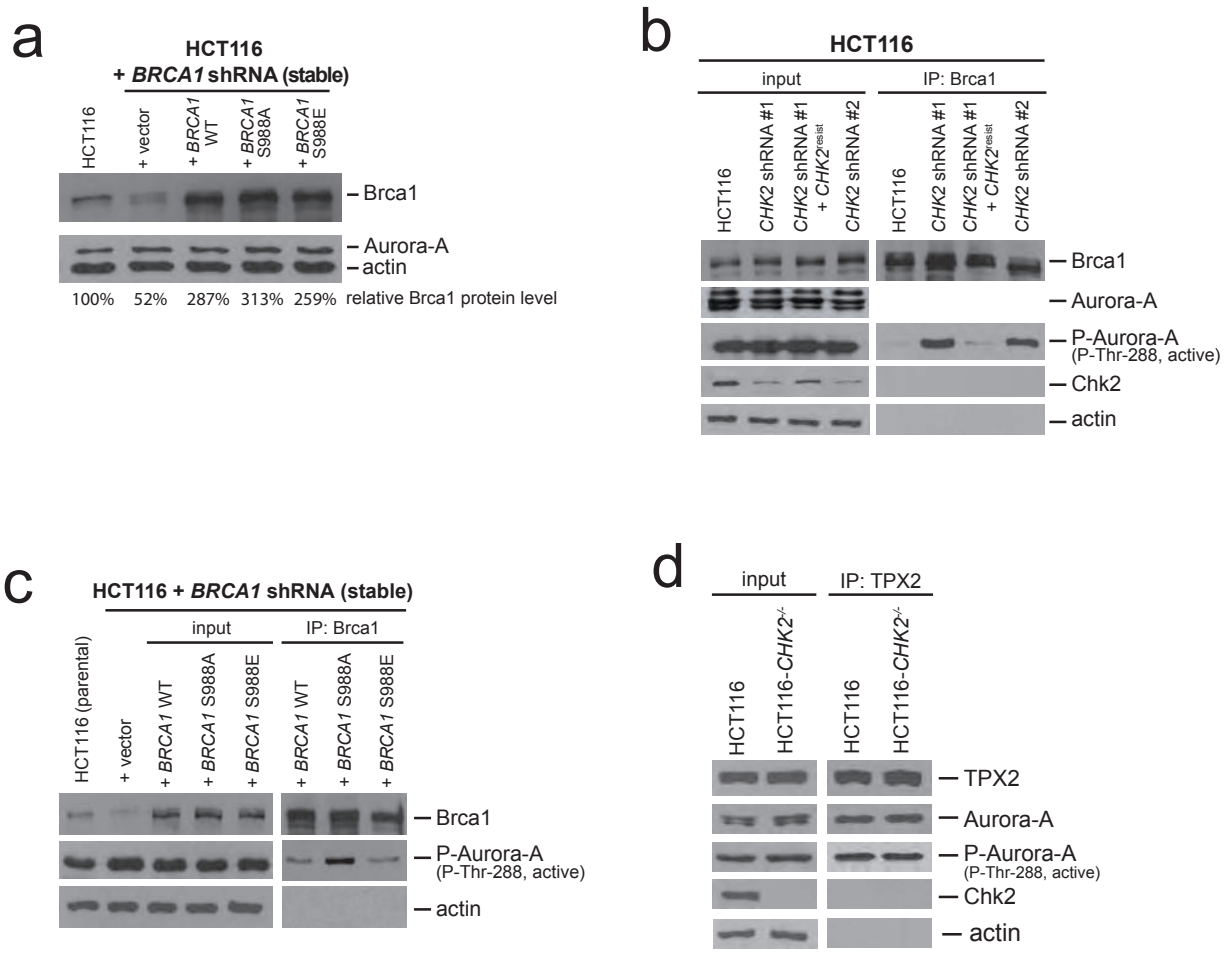

Supplementary Figure S7

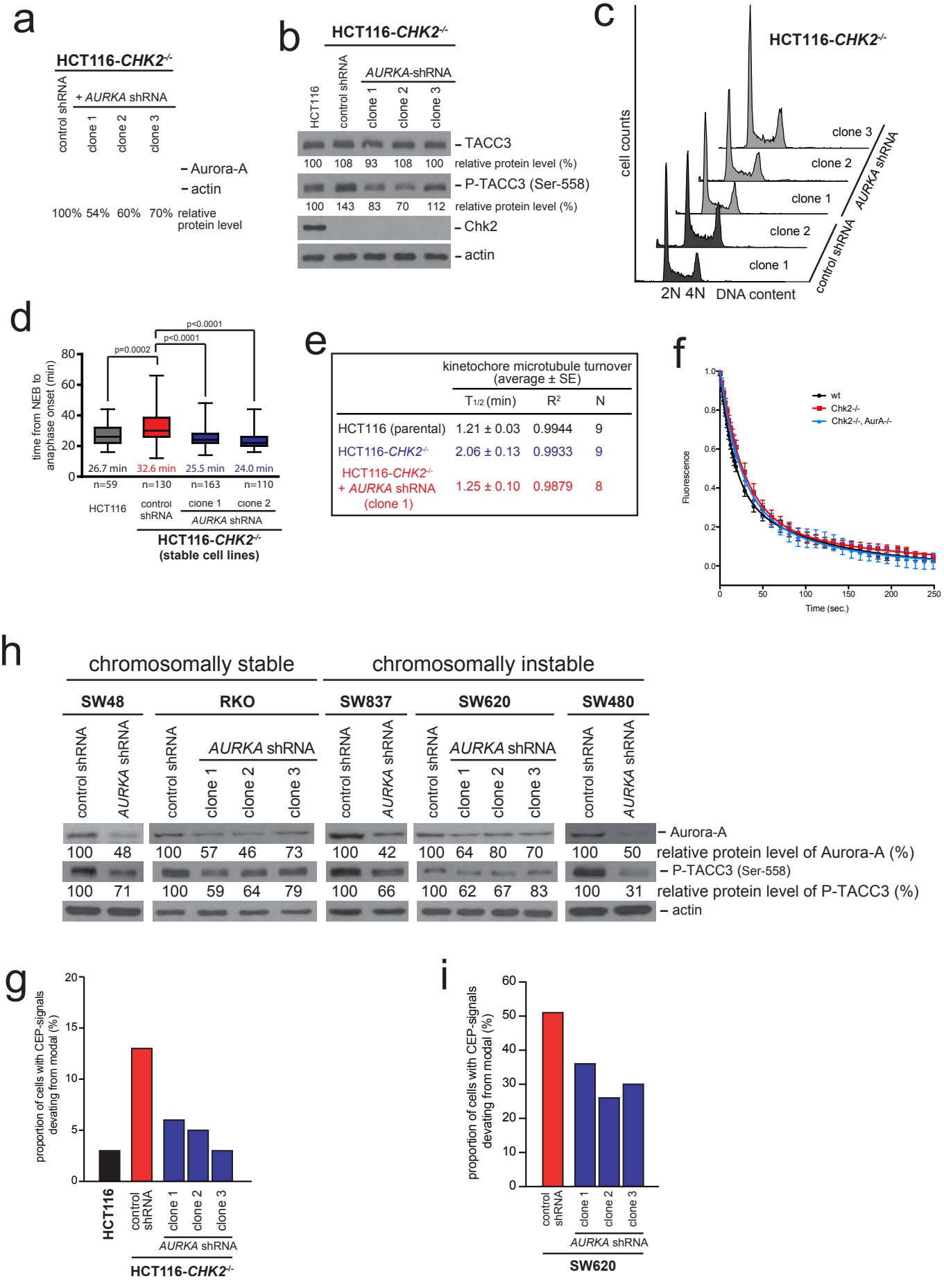

Supplementary Figure S8